antioxidants

MDPI

Article

Engineering *Collariella virescens* Peroxygenase for Epoxides Production from Vegetable Oil

Dolores Linde [1,†], Alejandro González-Benjumea [2,†], Carmen Aranda [3], Juan Carro [1], Ana Gutiérrez [2] and Angel T. Martínez [1,*]

[1] Centro de Investigaciones Biológicas "Margarita Salas" (CIB), Consejo Superior de Investigaciones Científicas (CSIC), E-28040 Madrid, Spain; lolalinde@cib.csic.es (D.L.); jcarro@cib.csic.es (J.C.)
[2] Instituto de Recursos Naturales y Agrobiología de Sevilla (IRNAS), Consejo Superior de Investigaciones Científicas (CSIC), E-41012 Seville, Spain; a.g.benjumea@irnas.csic.es (A.G.-B.); anagu@irnase.csic.es (A.G.)
[3] Johnson Matthey, Cambridge Science Park U260, Cambridge CB4 0FP, UK; carmen.aranda@matthey.com
* Correspondence: atmartinez@cib.csic.es; Tel.: +34-918373112
† These authors contributed equally to this work.

Abstract: Vegetable oils are valuable renewable resources for the production of bio-based chemicals and intermediates, including reactive epoxides of industrial interest. Enzymes are an environmentally friendly alternative to chemical catalysis in oxygenation reactions, epoxidation included, with the added advantage of their potential selectivity. The unspecific peroxygenase of *Collariella virescens* is only available as a recombinant enzyme (r*Cvi*UPO), which is produced in *Escherichia coli* for protein engineering and analytical-scale optimization of plant lipid oxygenation. Engineering the active site of r*Cvi*UPO (by substituting one, two, or up to six residues of its access channel by alanines) improved the epoxidation of individual 18-C unsaturated fatty acids and hydrolyzed sunflower oil. The double mutation at the heme channel (F88A/T158A) enhanced epoxidation of polyunsaturated linoleic and α–linolenic acids, with the desired diepoxides representing > 80% of the products (after 99% substrate conversion). More interestingly, process optimization increased (by 100-fold) the hydrolyzate concentration, with up to 85% epoxidation yield, after 1 h of reaction time with the above double variant. Under these conditions, oleic acid monoepoxide and linoleic acid diepoxide are the main products from the sunflower oil hydrolyzate.

Keywords: unspecific peroxygenase (UPO); *Collariella virescens*; heme access channel; protein engineering; epoxidation; unsaturated fatty acids; sunflower oil; process optimization

Citation: Linde, D.; González-Benjumea, A.; Aranda, C.; Carro, J.; Gutiérrez, A.; Martínez, A.T. Engineering *Collariella virescens* Peroxygenase for Epoxides Production from Vegetable Oil. *Antioxidants* **2022**, *11*, 915. https://doi.org/10.3390/antiox11050915

Academic Editor: Stanley Omaye

Received: 31 March 2022
Accepted: 3 May 2022
Published: 6 May 2022

1. Introduction

The oxirane ring of epoxides has been termed the "Lord of the chemical rings" [1] because of its high reactivity in the industrial production of bio-based chemicals and intermediates, including binder ingredients and resins. Epoxy resins comprise a group of cross-linkable materials, which polymerize with co-reactants (curing agents) into a matrix that can be used in a wide range of applications. Epoxy resins and curing agents usually contain more than one reaction site per molecule, to allow multiple crosslink reactions between them. Vegetable oils are one of the most important renewable feedstocks for a bio-based chemical industry [2–4]. The epoxides produced from oil fatty acids are possible ingredients for industrial resins (e.g., for board production), as long as they meet the required reaction selectivity and crosslinking properties.

Fatty acid epoxidation is industrially performed by the Prileschajew reaction [5] via percarboxylic acids, traditionally generated by strong acids [6], but also using formic acid [7] or ion-exchange resin [8]. Attempts to use milder conditions include chemoenzymatic lipase–H_2O_2 reactions on oils, free fatty acids, and their methyl esters [9–14], which maintain the drawbacks due to the use of peracids and direct enzymatic epoxidation. Some plant peroxygenases [15], cytochrome P450 monooxygenases [16], and fungal unspecific

peroxygenases (UPOs) [17] catalyze the direct epoxidation of (poly)unsaturated fatty acids. The latter enzymes present advantages related to their self-sufficiency (being independent of auxiliary proteins/modules and sources of reducing power) and secreted nature (being more stable than intracellular enzymes with monooxygenase activity) [18,19]. UPOs were known as aromatic peroxygenases [20], but, after first reports on their action on alkanes, fatty acids, and alcohols [21,22], numerous examples have shown their wide versatility on aliphatic compounds, including epoxidation reactions [23] and the name changed to unspecific peroxygenases (EC 1.11.2.1). The mechanism of this epoxidation reaction is illustrated in the catalytic cycle shown in Figure 1. This reaction is characterized by the presence of a modified compound II–substrate complex (Cpd II*), absent from the general peroxidase/peroxygenase catalytic cycle, that facilitates epoxide cyclization [19].

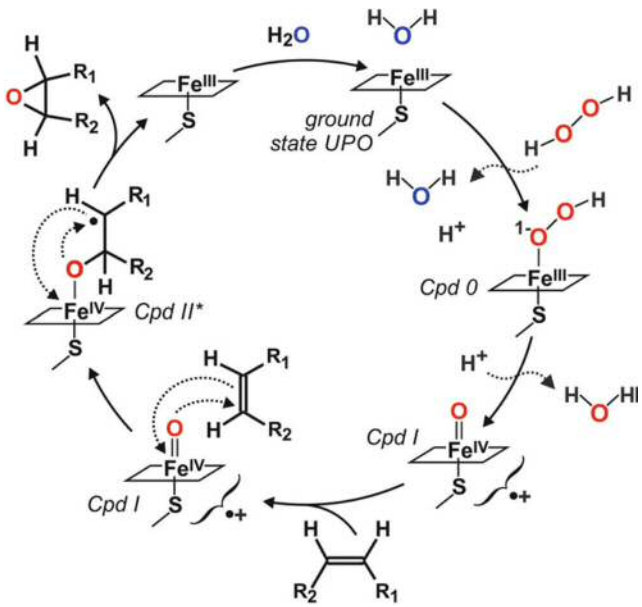

Figure 1. Proposed epoxidation cycle of UPO, showing activation of the ground state enzyme by H_2O_2, through hydroperoxo compound-0 (Cpd 0), to form reactive Cpd I able to epoxidize double bonds via a transient oxoferryl–substrate radical complex (Cpd II*). Reprinted from Ref. [19], 2020, Academic Press.

Recent studies on structure–function relationships in fatty-acid oxygenation by UPOs have revealed that the different peroxygenation patterns (enzyme regioselectivity) are ruled by the structure of the heme channel [24–26]. A good accessibility of the double bond of unsaturated fatty acids to the oxo group of the heme compound I (Cpd I formed after UPO activation by peroxide) is the key of the oxygenation reactions. In this way, different UPOs are able to produce different sets of oxygenated products (epoxy, hydroxy, and hydroxy–epoxy derivatives included) [17,21,27].

The UPO from the ascomycete *Collariella virescens* (syn. *Chaetomium virescens*; *Cvi*UPO) has been heterologously expressed in *Escherichia coli* and the recombinant enzyme (r*Cvi*UPO), isolated without any purification tag [28]. The obtained amounts are suitable for structure–function and (analytical scale) reaction optimization, making it a good starting point for future UPO studies. Moreover, r*Cvi*UPO shows good conversion of unsaturated fatty acids and, in contrast to other UPOs, generates epoxides as main products [25].

r*Cvi*UPO was already engineered by site-directed mutagenesis [25] in an initial attempt to mimic the heme environment of the UPO of related *Chaetomium globosum*, which efficiently epoxidizes unsaturated fatty acids [17]. Then, it was found that conversion of polyunsaturated omega 6 fatty acids (i.e., those with a double bond at the sixth position from the omega end) by the F88L variant of r*Cvi*UPO promoted diepoxidation [29]. This was explained by a wider heme access channel, facilitating epoxidation of two double bonds.

Increased epoxidation selectivity was also reported for the I153T variant of the *Marasmius rotula* enzyme [26], the first UPO heterologously expressed in *E. coli* (r*Mro*UPO) [30]. However, r*Mro*UPO has the disadvantage, compared to r*Cvi*UPO, of its much lower expression in *E. coli* as a soluble enzyme.

In the present work, we aimed to improve the conversion yield and selectivity of plant lipid epoxidation by r*Cvi*UPO via two different strategies: (i) enzyme engineering to achieve two epoxy groups per molecule, and (ii) analytical scale optimization of the reaction parameters to epoxidize hydrolyzed vegetable oil.

2. Materials and Methods

2.1. Production of Native Enzyme and Site-Directed Variants

The *Cvi*UPO sequence [31] was optimized for *E. coli* expression (using the software Optimizer) [32], synthesized, cloned, and produced as previously described [28]. The non-mutated recombinant (hereinafter native) enzyme was purified by two chromatographic steps in an Äkta (GE Healthcare, Chicago, IL, USA) fast liquid chromatography system. The first step was cation exchange chromatography with a HiTrap SPFF column (GE, Healthcare, Chicago, IL, USA) in 10 mM Tris (pH 7.4). The proteins, eluted as a single peak (recorded at 420 nm) with a gradient of the same buffer supplemented with 1 M NaCl, were concentrated in an Amicon 3K device (Sigma-Aldrich, Saint Louis, MO, USA). The second step (to ensure protein purity) was size-exclusion chromatography with a Superdex 75 column (10/300 GL; GE Healthcare, Chicago, IL, USA) in 10 mM Tris (pH 7.4) with 0.15 M NaCl.

A molecular model of the *Cvi*UPO structure was obtained at the Swiss-Model server (http://swissmodel.expasy.org, accessed on 1 March 2022) [33] with the structure of the first-reported [34] and crystallized [35] UPO of *Agrocybe aegerita* (*Aae*UPO) as a template (PDB entry 2YP1). This model was used for the design of four mutated variants with progressively enlarged heme access channels. The F88A and T158A single mutations were introduced in the *Cvi*UPO gene cloned in pET23a using the Expand Long Template PCR kit from Roche (Basel, Switzerland) and the following oligonucleotides as primers (direct sequences with the mutated codons underlined): F88A: 5′-ACT TAC ACC GTT CAG CAG CGT ATC GCG AGT TAC GGT GAA ACG-3′, T158A: 5′-AAC CGC CAT AAC CTG GCG GAA CAT GAT GCA TCT C-3′. For double mutation, the vector containing the *Cvi*UPO gene with the first mutation was used as a template. The PCR products were digested with *Dpn*I and transformed into *E. coli* DH5α for propagation. The gene of the 6Ala sextuple variant—including the L64A, I61A, F88A, T157A, T158A, and T165A mutations—was synthesized by ATG-biosynthetics GmbH (Merzhausen, Germany). All the variants were produced in *E. coli* as active cytosolic enzymes, and purified as described above for the native r*Cvi*UPO.

Enzyme purity was confirmed under denaturing conditions by 12% polyacrylamide gel electrophoresis (PAGE) in the presence of 0.1% sodium dodecyl sulfate (SDS) and 1% mercaptoethanol [36]. Proper folding and binding of the cofactor were verified by analyzing the UV–visible spectrum of the resting state of the enzymes in 10 mM Tris (pH 7.4) using a Cary 60 spectrophotometer (Agilent, Santa Clara, CA, USA). Additionally, formation of the characteristic complex between reduced heme-thiolate enzymes (ferrous form) and carbon monoxide (CO) was assessed in 0.2 M phosphate (pH 8) after addition of $Na_2S_2O_4$ and CO flushing. UPO concentrations were calculated using the r*Cvi*UPO molar extinction coefficient of ε_{420} = 114.2 $mM^{-1} \cdot cm^{-1}$ [28].

2.2. Enzyme Kinetics

Optimal pH values for oxidation of several UPO substrates—namely veratryl and benzyl alcohols (10 mM) and naphthalene (1 mM) from Merck (Darmstadt, Germany) and 2,2′-azino-bis(3-ethylbenzothiazoline-6-sulfonic acid) (ABTS; 2 mM) from Boehringer Mannheim (Mannheim, Germany)—by the native r*Cvi*UPO and its variants were analyzed

in the range of pH 2–10 using 0.2 M Britton–Robinson buffer, at 24 °C, in the presence of 1 mM H_2O_2.

Kinetic curves for the above enzyme-reducing substrates were obtained (with spectrophotometric assays) from the initial (10–30 s) increase of product absorbance, using a Thermo Spectronic UV–visible spectrophotometer (Waltham, MA, USA) at the optimal pH for each enzyme and substrate. Oxidation of veratryl alcohol (0.09–50 mM, in 0.1 M acetate, pH 3 or 5) was followed at 310 nm (ε_{310} = 9300 $M^{-1}\cdot cm^{-1}$), benzyl alcohol (0.3–50 mM, in 0.1 M Tris, pH 6) at 280 nm (ε_{280} = 1400 $M^{-1}\cdot cm^{-1}$), naphthalene (0.03–2 mM, in 0.1 M tartrate, pH 6, with 5% ethanol) at 303 nm (ε_{303} = 2030 $M^{-1}\cdot cm^{-1}$), and ABTS (0.04–5 mM in 0.1 M acetate, pH 4) at 436 nm (ε_{436} = 29,300 $M^{-1}\cdot cm^{-1}$). Reactions (1 mL) were triggered by the addition of 1 mM or 24 mM H_2O_2. Kinetic curves for H_2O_2 were obtained with different peroxide concentrations (0.5–30 mM, in 0.1 M acetate, pH 4) in the presence of 2.5 mM ABTS whose (one-electron) oxidation was monitored at 436 nm (as explained above) for activity estimation (note that two moles of ABTS are oxidized by each mole of peroxide), and the H_2O_2 K_m values were obtained.

Kinetic curves for oleic acid oxidation (estimated chromatographically) were obtained by varying the concentration from 12.5 μM to 1.6 mM substrate, in 50 mM phosphate (pH 7) containing 20% acetone (*v*/*v*). Reactions (1 mL) were triggered by the addition of 24 mM H_2O_2 and stopped after 1 min by vigorous shaking with 100 μL of 0.1 M sodium azide. The oxygenated products were extracted, analyzed by gas chromatography–mass spectrometry (GC-MS) as described below, and their total abundance was used for the calculation of kinetic constants. All reactions were carried out in triplicate.

Curve-fit and data analysis for kinetic constant estimation were carried out using Sigma Plot 11.0. Michaelis–Menten constant (K_m) and turnover number (catalytic constant, k_{cat}), and their standard errors were obtained by non-linear fitting the k_{obs} values to Equation (1) (Michaelis–Menten model) except for (i) ABTS oxidation by r*Cvi*UPO and T158A using 1 mM H_2O_2; (ii) ABTS oxidation by F88A (using either 1 mM or 24 mM H_2O_2); (iii) benzyl alcohol oxidation by F88A and F88A/T158A using 1 mM H_2O_2; (iv) oleic acid oxidation by the F88A, F88A/T158A, and 6Ala variants; (v) H_2O_2 reduction (in presence of 2.5 mM ABTS) by r*Cvi*UPO and T158A variant, where enzyme inhibition was observed, being therefore adjusted to Equation (2) (with the k_i inhibition constant being the concentration producing half maximum inhibition); and (vi) benzyl alcohol oxidation by r*Cvi*UPO and T158A using 1 mM H_2O_2 that was adjusted to Equation (3) (Hill model with n_H providing a measurement of the cooperativity of the substrate binding to the enzyme, and $K_{0.5}$ being the substrate concentration for half saturation).

$$f = \frac{k_{cat}\,S}{K_m + S} \quad (1)$$

$$f = \frac{k_{cat}}{1 + \frac{K_m}{S} + \frac{S}{k_i}} \quad (2)$$

$$f = \frac{y_0 + k_{cat}S^{n_H}}{{K_{0.5}}^{n_H} + S^{n_H}} \quad (3)$$

2.3. Epoxidation of Individual Fatty Acids and Oil Hydrolyzate

For evaluating the UPO epoxidation ability, the following 18-C unsaturated fatty acids (from Sigma-Aldrich, Saint Louis, MO, USA) were used as substrates: oleic (*cis*-9-octadecenoic, C18:1), linoleic (*cis*,*cis*-9,12-octadecadienoic, C18:2), and α-linolenic (*cis*,*cis*,*cis*-9,12,15-octadecatrienoic, C18:3) acids. Reactions running for 30 min were performed using 0.1 mM substrate, 0.25 or 0.4 μM enzyme (C18:1/C18:3 or C18:2 reactions, respectively), and 1.25 mM H_2O_2 in 50 mM phosphate (pH 7), at 30 °C in the presence of 20% acetone (for better substrate solubilization). For more complete characterization, epoxyoleic acid was prepared in larger scale (50 mL) reactions and purified by silica gel (60–200 μm) column chromatography using hexane–EtOAc (10:1 → 5:1) as the mobile phase.

Oil hydrolyzate was assayed for epoxide production as a more economical and sustainable substrate than pure fatty acids. Sunflower oil (supplied by Cargill in the frame of the project SusBind, https://susbind.eu, accessed on 1 March 2022) was saponified and the hydrolyzed fatty acids extracted at acidic pH as previously described [37]. Initial reactions were performed for 30 min using 0.1 mM hydrolyzate, 0.25 μM enzyme, and 1 mM H_2O_2 in 50 mM phosphate buffer (pH 7) containing 20% acetone (conditions similar to those used with individual fatty acids). In further reactions, up to 10 mM oil hydrolyzate was used, and the effect of several variables was studied including: pH 5.5/7.0, 20/30% acetone cosolvent, 0.25/0.50 μM enzyme (resulting in 100–400 substrate/enzyme (S/E) molar ratio), 1–100 mM H_2O_2 (resulting in 1.0–6.8 equivalents per fatty-acid double bond) added with a syringe pump, and 30/60 min reaction time. Given the results obtained with individual fatty acids, the F88A/T158A variant was selected for hydrolyzate reactions, compared with native r*Cvi*UPO. Epoxidation yields were calculated taking into account the epoxidation degree, the number of unsaturations, and the reaction conversion for each substrate. In all cases, control experiments were carried out under the same conditions (H_2O_2 included), but in the absence of enzyme.

2.4. GC-MS Analyses

Products (and unreacted substrates) from the above reactions were liquid–liquid extracted with methyl *tert*-butyl ether (Sigma-Aldrich, Saint Louis, MO, USA), which was evaporated under a N_2 stream. *N*,*O*-Bis(trimethylsilyl)trifluoroacetamide (Supelco, Bellefonte, PA, USA) was used to prepare trimethylsilyl derivatives. The GC-MS analyses were performed with an Agilent (Santa Clara, CA, USA) GC-MS QP2020 Ultra equipment using a fused-silica DB-5HT 30 m capillary column from J&W Scientific (Folsom, CA, USA). The oven was heated from 120 °C (1 min) to 300 °C (15 min) at 5 °C min^{-1}. The injector and transfer line were kept at 300 °C. Compounds were identified by mass fragmentography and comparison of their mass spectra with those of authentic standards. Quantifications were obtained from total-ion peak areas (after deconvolution when partial overlapping was observed) and molar response factors of the same or similar compounds.

2.5. Chiral Analyses

Chiral analyses of epoxides of oleic acid were performed after derivatization into methyl esters (using trimethylsylyldiazomethane from Sigma-Aldrich, Saint Louis, MO, USA) with a Shimadzu (Kyoto, Japan) i-Prominence 2030C high-performance liquid chromatography (HPLC) equipment using an OB-H (250 × 4.6 cm, 5 μm particle) column from Daicel (Osaka, Japan). Compounds were eluted with hexane–^{i}PrOH-AcOH (99.65:0.3:0.05), at a flow rate of 0.8 mL·min^{-1} and monitored at 202 nm. Enantiomer assignment was done following the reported literature [38].

3. Results and Discussion

3.1. Design and Catalytic Characterization of rCviUPO Variants

Previous results with r*Cvi*UPO variants [25] led us to study the further broadening of its heme channel. For simplicity, the residues surrounding heme access were mutated into alanines; two simple (F88A and T158A), one double (F88A/T158A), and one sextuple (I61A/L64A/F88A/T157A/T158A/T165A) variants were designed (Figure 2). The variants were expressed as soluble active enzymes, and purified by a combination of cation exchange and size-exclusion chromatography [28]. In all cases, electrophoretic homogeneity was attained, as revealed by SDS-PAGE (Figure S1). Moreover, correct incorporation of the heme-thiolate group was confirmed by spectrophotometric analysis of the enzyme resting state, with the reduced enzyme complex with CO (Figure S2 main panels and insets, respectively) exhibiting characteristic maxima around 420 and 440 nm, respectively.

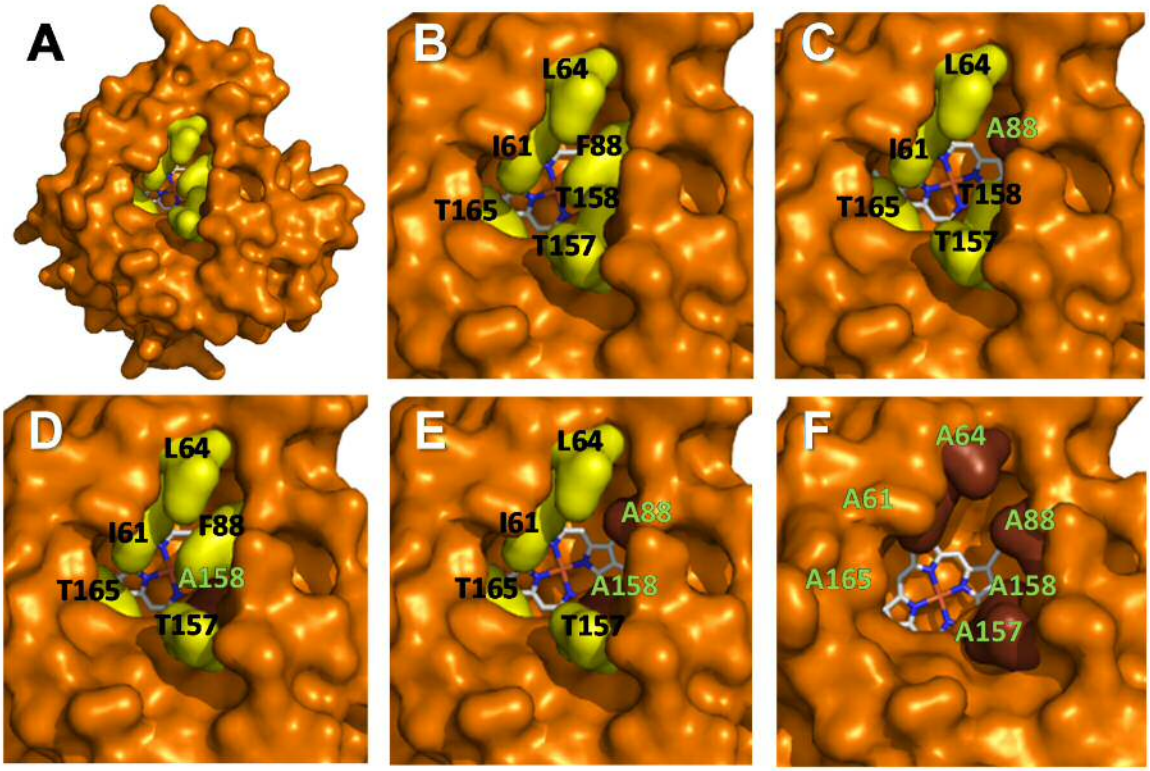

Figure 2. Solvent-access surface in *Cvi*UPO molecular model (**A**), and detail of the access channel to the heme cofactor (as CPK-colored sticks) in the native enzyme (**B**) and its F88A (**C**), T158A (**D**), F88A/T158A (**E**), and 6Ala (**F**) variants. Those residues to be mutated (black labels) have yellow surfaces; the already-introduced alanines (yellow labels in **C**–**F**) show brown surfaces.

First, the optimal pH for oxidation of four peroxidase/peroxygenase substrates was determined for the native r*Cvi*UPO and variants (Figure S3). Kinetic curves and constants were first obtained with 1 mM H_2O_2 as the enzyme-oxidizing substrate (Figure S4A–D and Table S1, respectively). Catalytic constants for H_2O_2 were determined using 2.5 mM ABTS as co-substrate. It was observed that the native r*Cvi*UPO and its T158A variant are inhibited by high H_2O_2 concentrations (Figure S4E), with inhibition constants (k_i) of 5.6 mM and 1.8 mM, respectively (Table 1). The r*Cvi*UPO variants showed decreased catalytic efficiency for the enzyme-oxidizing substrate, due to 6- to 15-fold lower affinity for H_2O_2 than the native r*Cvi*UPO, with all the K_m values > 1 mM (native r*Cvi*UPO included). Therefore, the k_{cat} values for the different enzyme-reducing substrates would be often undervalued under the above conditions.

Table 1. Kinetic constants for H_2O_2 reaction with native r*Cvi*UPO and variants.

	K_m (μM)	k_{cat}/K_m ($s^{-1} \cdot mM^{-1}$)	k_i (μM)
Native	1600 ± 468	374 ± 129	5580 ± 1800
F88A	16,300 ± 2900	29 ± 6	-
T158A	23,800 ± 13,700	127 ± 99	1790 ± 1000
F88A/T158A	9370 ± 880	55 ± 6	-
6Ala	14,800 ± 1600	0.7 ± 0.1	-

Measured in 100 mM acetate (pH 4) with 2.5 mM ABTS as reducing substrate. The high error values in the r*Cvi*UPO and T158A constants originate from the use of Equation (2) due to observed inhibition (Figure S4E) that, despite the good adjustments (R^2 values of 0.988 and 0.997, respectively), has limited precision in predicting kinetic constants.

For this reason, second sets of kinetic curves and constants were obtained using 24 mM H_2O_2 (Figure S4F–I and Table S2, respectively) for better enzyme saturation. Under these conditions, increased catalytic efficiency of the simple and double variants could

be observed. For F88A/T158A, up to 75-, 10- and 4-fold increases (with respect to native r*Cvi*UPO) were found for naphthalene, veratryl alcohol/ABTS, and benzyl alcohol, respectively. The broadest channel variant 6Ala showed improved affinity with all substrates, but often also lower reaction rates, resulting in lower catalytic efficiency.

Concerning oleic acid oxygenation by native r*Cvi*UPO and variants (Table 2), smaller differences in kinetic constants than those found for the other substrates were generally observed. Among them, it is worth mentioning the following: (i) a 50% increase of catalytic efficiency by the F88A/T158A variant, due to moderate improvements in both affinity and turnover; and (ii) over 5-fold reduction in catalytic efficiency by the F88A and 6Ala variants.

Table 2. Kinetic constants for oleic acid oxygenation by native r*Cvi*UPO and variants.

	k_{cat} (s^{-1})	K_m (μM)	k_{cat}/K_m ($s^{-1} \cdot mM^{-1}$)	k_i (μM)
Native	12.6 ± 0.3	58.8 ± 6.0	214 ± 53	-
F88A	10.5 ± 1.7	278.0 ± 49.0	38 ± 9	1120 ± 400
T158A	21.0 ± 1.1	89.0 ± 16.4	184 ± 35	-
F88A/T158A	16.5 ± 0.5	51.6 ± 5.4	319 ± 35	2900 ± 610
6Ala	16.6 ± 3.6	399.0 ± 94.6	42 ± 13	1360 ± 710

The kinetic constants were measured in 50 mM phosphate buffer (pH 7) in the presence of 24 mM H_2O_2.

The structural changes introduced in the new variants generated some catalytic improvements in oxygenation ability, particularly with the F88A/T158A variant compared with the native r*Cvi*UPO, as shown using naphthalene and oleic acid. These results indicate that this heme channel variant is a potentially interesting epoxidation biocatalyst, as described below.

3.2. Fatty-Acid Oxygenation Patterns by rCviUPO and Heme-Channel Variants

GC-MS analyses revealed different oxygenation products in the reactions of oleic, linoleic, and α-linolenic acids with r*Cvi*UPO and its F88A, T158A, F158A/T158A, and 6Ala variants (see chromatographic profiles in Figures S5–S7). The relative abundance of the different product classes—namely 9-epoxy, 12-epoxy, 15-epoxy, diepoxy, OH-/keto, and OH-epoxy derivatives—together with the conversion percentage and the epoxidation yield, are indicated in Table 3. In all cases, up to 88–99% conversions were attained with the native enzyme and its variants. Due to the native r*Cvi*UPO selectivity towards mono-epoxidation, its epoxidation yield decreased from oleic acid (71%) to α-linolenic acid (32%). However, the changes introduced in the mutated variants improved the epoxidation yields, reaching 93% with oleic acid (T158A), 90% with linoleic acid (F88A/T158A), and 60% with α-linolenic acid (F88A/T158A).

Concerning the products, chromatograms in Figure 3 illustrate the most interesting reactions: (i) preferential epoxidation of oleic acid by the 6Ala variant (B) without the fatty acid hydroxylated derivatives (at the allylic position) formed by the native enzyme (A), and (ii) preferential diepoxidation (>80% of products) of linoleic and α–linolenic acids (D and F, respectively) by the F88A/T158A variant instead of the mono-epoxidation produced by the native enzyme (C and E, respectively).

Table 3. Fatty acid conversion, percentages of main products, and epoxidation yield (calculated with respect to the total number of double bonds present) in the reactions of 18-C fatty acids with native r*Cvi*UPO and four heme channel variants.

	Conversion	Products (%)						Epoxidation
	(%)	15-Epoxy	12-Epoxy	9-Epoxy	Diepoxy	OH/Keto	OH-Epoxy	Yield (%)
C18:1								
Native	96	-	-	71	-	28	1	71
F88A	97	-	-	69	-	6	25	91
T158A	98	-	-	87	-	5	8	93
F88A/T158A	95	-	-	63	-	13	24	82
6Ala	96	-	-	96	-	4	-	92
C18:2								
Native	97	-	56	10	-	8	26	45
F88A	98	-	15	2	46	12	25	66
T158A	88	-	23	17	29	27	4	43
F88A/T158A	99	-	4	-	81	-	15	90
6Ala	99	-	-	25	64	-	11	81
C18:3								
Native	96	77	6	2	-	-	15	32
F88A	98	16	6	4	53	8	13	47
T158A	98	26	30	17	3	20	3	27
F88A/T158A	99	2	3	-	82	-	13	60
6Ala	99	17	35	16	10	16	6	47

The products from 30 min reactions of 0.25 μM or 0.40 μM enzyme with C18:1/C18:3 and C18:2, respectively, in 50 mM phosphate buffer (pH 7) containing 20% acetone, were extracted with methyl *tert*-butyl ether and analyzed by GC-MS as trimethylsilyl derivatives.

Finally, encouraged by the recently reported enantioselectivity of fatty acid monoepoxidations with UPOs [24,25], reactions with oleic acid were carried out at a larger scale, and the epoxyoleic products were purified prior to chiral HPLC analysis. The 6Ala variant was selected due to its high regioselectivity to the epoxide, together with the F88A/T158A variant as the best UPO in terms of the overall epoxidation yield with all substrates (and native r*Cvi*UPO for comparative purposes). The results obtained (Figure S8) revealed only low enantioselectivity with the three enzymes (*ee* 0–40%), although an inversion of the configuration of the main enantiomer was produced between the F88A/T158A and 6Ala variants (70% *S*/*R* and 60% *R*/*S*, respectively).

3.3. Optimization of Hydrolyzed Sunflower Oil Epoxidation

After testing the r*Cvi*UPO variants on individual unsaturated fatty acids, the goal was to accomplish the epoxidation of hydrolyzed vegetable oil. For this purpose, a sunflower oil hydrolyzate was used as substrate, and several parameters—including substrate, enzyme, and H_2O_2 concentrations, among others—were optimized.

Firstly, reactions under the same conditions used with pure fatty acids were performed on hydrolyzed sunflower oil (0.1 mM) using native r*Cvi*UPO and its F88A/T158A variant (Figure 4A,B, respectively). Both enzymes were able to convert the oil unsaturated fatty acids with similar regioselectivity, forming (i) monoepoxides from oleic acid and linoleic acid (at 9 and 12 positions) as main products, (ii) two diepoxy isomers (*anti* and *syn*) from linoleic acid, more abundant in the F88A/T158A reaction; and (iii) small amounts of hydroxy- and hydroxy-epoxy derivatives of oleic acid and linoleic acids, together with some minor products.

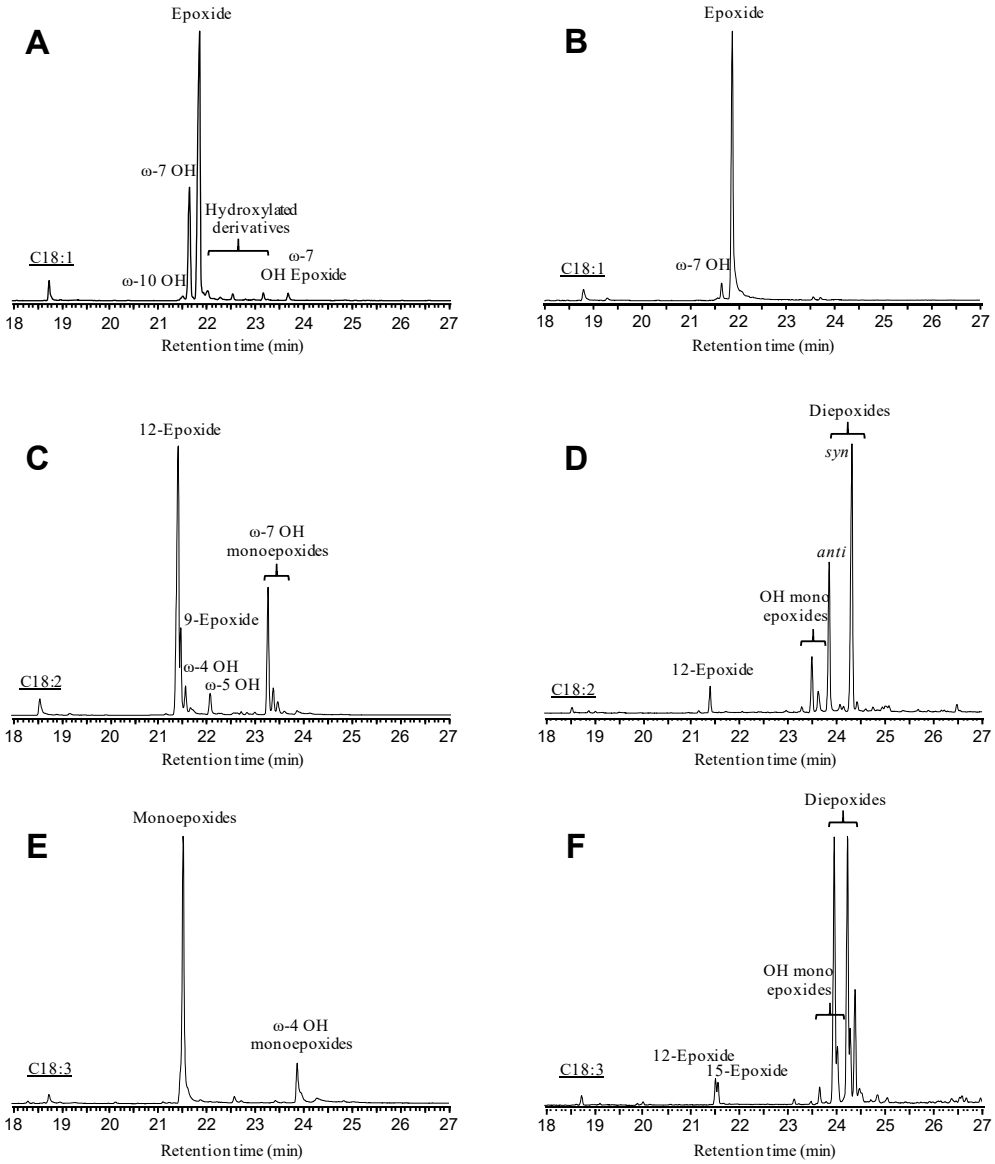

Figure 3. GC-MS profiles of selected epoxidation reactions of: (i) oleic acid (C18:1) treated with the 6Ala variant (**B**) compared with native r*Cvi*UPO (**A**), (ii) linoleic acid treated with the F88A/T158A variant (**D**) compared with the native r*Cvi*UPO (**C**), and (iii) α–linolenic acid treated with the F88A/T158A variant (**F**) compared with the native r*Cvi*UPO (**E**) (see Figures S5–S7 for the whole set of reactions). Mixtures containing 0.1 mM substrate, 0.25–0.40 μM enzyme, and 1.25 mM H_2O_2 were incubated for 30 min, extracted, and derivatized before GC-MS analysis.

Then, differences in the epoxidation yields were observed when varying the enzyme dose, using different substrate/enzyme (S/E) molar ratios. As shown in Table 4 (entries 1–6), increasing the r*Cvi*UPO dose did not result in improved epoxidation yield, but doubling the amount of F88A/T158A (0.5 μM, S/E ratio 200) yielded higher amounts of diepoxides from linoleic acid (the epoxidation of oleic acid was retained); consequently, a better epoxidation yield (72%) was attained. Nevertheless, a 1 μM dose of the double variant (S/E ratio 100) produced virtually the same epoxidation profile. Therefore, optimal 400 and 200 S/E ratios were fixed for further scale up with r*Cvi*UPO and its double variant, respectively.

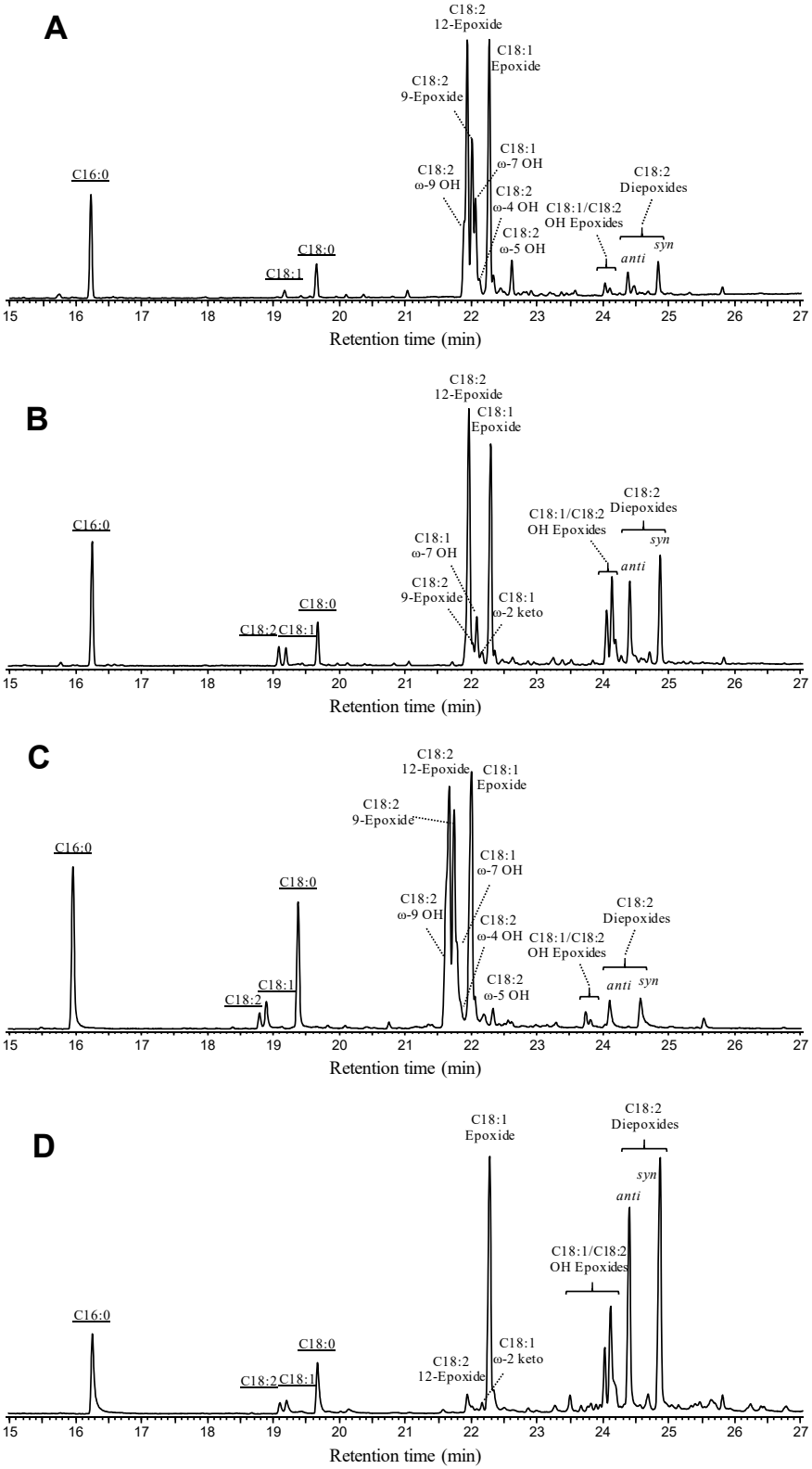

Figure 4. GC-MS profiles of UPO reactions with sunflower oil hydrolyzate. (**A**,**B**) Initial treatment of 0.1 mM oil hydrolyzate with 0.25 μM r*Cvi*UPO and its F88A/T158A variant, respectively, for 30 min in 50 mM phosphate (pH 7) containing 20% acetone and 1 mM H_2O_2. (**C**,**D**) Optimized treatment of 10 mM oil hydrolyzate with 25 μM r*Cvi*UPO and 50 μM F88A/T158A for 60 min in 50 mM phosphate buffer (pH 7) containing 30% acetone and 25 mM H_2O_2.

Table 4. Optimizing epoxidation yield (as percentage of the number of total double bonds present) in treatment of sunflower oil hydrolyzate with the selected r*Cvi*UPO variant (F88A/T158A) compared with native enzyme, by varying reaction parameters—such as substrate loading (mM), enzyme dose (μM), substrate/enzyme (S/E) molar ratio, acetone content (*v*/*v* %), H_2O_2 dose (mM and equivalents per fatty-acid double bond), and time (min)—under different combinations (entries 1–17).

Entry	Preparation	Substrate, mM	Enzyme, μM (S/E Ratio)	Acetone, %	H_2O_2, mM (Equiv)	Time, min	Epoxidation Yield, %
1	native	0.1	0.25 (400)	20	1 (6.8)	30	54
2	native	0.1	0.5 (200)	20	1 (6.8)	30	52
3	native	0.1	1 (100)	20	1 (6.8)	30	53
4	F88A/T158A	0.1	0.25 (400)	20	1 (6.8)	30	59
5	F88A/T158A	0.1	0.5 (200)	20	1 (6.8)	30	72
6	F88A/T158A	0.1	1 (100)	20	1 (6.8)	30	75
7	native	5	12.5 (400)	20	50 (6.8)	30	8
8	native	5	12.5 (400)	20	50 (6.8)	60	28
9	F88A/T158A	5	25 (200)	20	50 (6.8)	30	35
10	F88A/T158A	5	25 (200)	20	50 (6.8)	60	84
11	native	10	25 (400)	20	100 (6.8)	60	37
12	native	10	25 (400)	30	100 (6.8)	60	56
13	F88A/T158A	10	50 (200)	20	100 (6.8)	60	40
14	F88A/T158A	10	50 (200)	30	100 (6.8)	60	79
15	F88A/T158A	10	50 (200)	30	50 (3.4)	60	78
16	F88A/T158A	10	50 (200)	30	25 (1.7)	60	85
17	F88A/T158A	10	50 (200)	30	15 (1.0)	60	44

However, when the substrate loading was increased to 5 mM (Table 4 entries 7–10), its conversion rate decayed with both enzymes within 30 min reactions. Therefore, an extension of the reaction time up to 60 min was needed to reverse the epoxidation performance with the F88A/T158A variant at the initial reaction level (entry 10). In fact, the reaction time becomes critical in UPO epoxidation of fatty acids when the substrate concentration is close to the solvent saturation [28].

Finally, with 10 mM substrate loading (Table 4 entries 11–17), the importance of the substrate solubilization was revealed by comparing the epoxidation yields with 20% and 30% acetone cosolvent. With both enzymes, 20% acetone resulted in low conversion and epoxidation yields (longer times did not improve the results). However, the complete solubilization of substrates using 30% acetone improved the epoxidation yield, especially with the double variant (entry 14) forming mono and diepoxide amounts similar to those observed in reactions with a lower substrate concentration.

With the enzyme dose, amount of co-solvent, and reaction time already optimized, assays were conducted to determine the lowest dose of H_2O_2 that enables the production of the highest epoxidation yield. As depicted in Table 4, the highest epoxidation yield (85%) was attained using only 1.7 equivalents of this oxidizer (entry 16), compared with the 6.8 (used in most previous assays) and 3.4 (entry 15) equivalents, while adding a stoichiometric amount of H_2O_2 (entry 17) led to a decrease in epoxidation yield (to only 44%).

The pattern of oxygenation products produced under optimized conditions (Figure 4C,D) was similar to that obtained previously, with linoleic acid diepoxides and oleic acid monoepoxide as the main products in the F88A/T158A reactions. No triepoxides were detected in any of the reactions, due to the low α–linolenic acid content of sunflower oil [37]. The above results reveal the remarkable potential of the r*Cvi*UPO double variant for epoxidizing sunflower oil hydrolyzate, demonstrating a much higher conversion yield than the native enzyme.

4. Conclusions

Opening the r*Cvi*UPO heme access channel allowed us to improve the epoxidation activity of this enzyme, selected for protein engineering in *E. coli*. In this way, the variant with the widest channel, after a sextuple mutation, yielded the highest epoxidation of oleic acid to the corresponding monoepoxide (with less than 5% of other oxygenation products). In contrast, a double variant (F88A/T158A) produced the best conversion of both linoleic and α–linolenic acids with diepoxides, of interest as crosslinking molecules, representing > 80% of products. Under the same conditions used for individual fatty acids, the double variant also converted hydrolyzed sunflower oil with a higher epoxidation yield than the native enzyme. Moreover, process optimization permitted us to increase (×100) the hydrolyzate concentration, epoxidizing 85% of double bonds after 1 h of reaction time with the mutated double variant. UPO engineering, strongly limited in the past by difficulties in heterologous expression of these enzymes in adequate hosts, is a requirement for developing the large repertoire of reactions of industrial relevance suggested in recent reviews [23,39–45] on an enzyme family of the highest interest for selective oxyfunctionalization reactions [46].

Supplementary Materials: The following supporting information can be downloaded at https://www.mdpi.com/article/10.3390/antiox11050915/s1. Kinetic constants for substrate oxidation by native r*Cvi*UPO and variants in the presence of 1 mM and 24 mM H_2O_2 (Table S1 and Table S2, respectively); SDS-PAGE of purified native rCviUPO and variants (Figure S1); UV–visible spectra of resting states and CO complexes of rCviUPO and variants (Figure S2); Effect of pH on the oxidation of different substrates (Figure S3); Kinetic curves for different UPO reducing substrates and H_2O_2 (Figure S4); GC-MS analyses of oleic, linoleic, and α–linolenic acids reactions with CviUPO and four heme channel variants (Figure S5, Figure S6 and S7, respectively); and Chiral HPLC analysis of oleic acid epoxide (Figure S8).

Author Contributions: Conceptualization, D.L., C.A. and A.T.M.; methodology, D.L., A.G.-B., C.A. and J.C.; formal analysis, D.L., A.G.-B. and C.A.; investigation, D.L., A.G.-B., C.A. and J.C.; resources, A.G. and A.T.M.; data curation, D.L. and A.G.-B.; writing—original draft preparation, D.L., A.G.-B. and J.C.; writing—review and editing, A.G. and A.T.M.; supervision, A.T.M. and A.G.; project administration, A.T.M.; funding acquisition, A.G. and A.T.M. All authors have read and agreed to the published version of the manuscript.

Funding: This research was funded by BioBased Industries Joint Undertaking under the European Union's Horizon 2020 Research and Innovation Programme, grant number 792063 (SusBind project; https://susbind.eu; to A.G and A.T.M.); the BIO2017-86559-R project of the Spanish Ministry of Science and Innovation (co-financed by FEDER funds; to A.T.M.); the PID2020-118968RB-100 project by the Spanish MCIN/AEI/10.13039/501100011033 (to A.G.); the CSIC projects PIE-202040E185 (to A.G.) and PIE-202120E019 (to A.T.M.); the CSIC SusPlast platform (to A.T.M.); and the CSIC program for the Spanish Recovery, Transformation, and Resilience Plan funded by the Recovery and Resilience Facility of the European Union, established by the Regulation (EU) 2020/2094.

Institutional Review Board Statement: Not applicable.

Informed Consent Statement: Not applicable.

Data Availability Statement: All data underlying this article are available in the main publication and in its Supplementary Material online.

Acknowledgments: We acknowledge support for the publication fee by the CSIC Open Access Publication Support Initiative through its Unit of Information Resources for Research (URICI).

Conflicts of Interest: The authors declare no conflict of interest.

References

1. Meng, Y.; Taddeo, F.; Aguilera, A.F.; Cai, X.; Russo, V.; Tolvanen, P.; Leveneur, S. The Lord of the chemical rings: Catalytic synthesis of important industrial epoxide compounds. *Catalysts* **2021**, *11*, 7. [CrossRef]
2. Biermann, U.; Friedt, W.; Lang, S.; Lühs, W.; Machmüller, G.; Metzger, U.O.; Klaas, M.R.; Schäfer, H.J.; Schneider, M.P. New syntheses with oils and fats as renewable raw materials for the chemical industry. In *Biorefineries-Industrial Processes and Products*; Kamm, B., Gruber, P.R., Kamm, M., Eds.; Wiley-VCH Verlag GmbH: Weinheim, Germany, 2006; pp. 253–289.

3. Corma, A.; Iborra, S.; Velty, A. Chemical routes for the transformation of biomass into chemicals. *Chem. Rev.* **2007**, *107*, 2411–2502. [CrossRef] [PubMed]
4. Biermann, U.; Bornscheuer, U.; Meier, M.A.R.; Metzger, J.O.; Schäfer, H.J. Oils and Fats as Renewable Raw Materials in Chemistry. *Angew. Chem. Int. Ed.* **2011**, *50*, 3854–3871. [CrossRef] [PubMed]
5. Prileschajew, N. Oxydation ungesättigter Verbindungen mittels organischer Superoxyde. *Ber. Dtsch. Chem. Ges.* **1909**, *42*, 4811–4815. [CrossRef]
6. Zheng, J.L.; Wärnå, J.; Salmi, T.; Burel, F.; Taouk, B.; Leveneur, S. Kinetic modeling strategy for an exothermic multiphase reactor system: Application to vegetable oils epoxidation using Prileschajew method. *AIChE J.* **2016**, *62*, 726–741. [CrossRef]
7. Santacesaria, E.; Tesser, R.; Di Serio, M.; Turco, R.; Russo, V.; Verde, D. A biphasic model describing soybean oil epoxidation with H2O2 in a fed-batch reactor. *Chem. Eng. J.* **2011**, *173*, 198–209. [CrossRef]
8. Sinadinovic-Fiser, S.; Jankovic, M.; Borota, O. Epoxidation of castor oil with peracetic acid formed in situ in the presence of an ion exchange resin. *Chem. Eng. Process.* **2012**, *62*, 106–113. [CrossRef]
9. Björkling, F.; Frykman, H.; Godtfredsen, S.E.; Kirk, O. Lipase catalyzed synthesis of peroxycarboxylic acids and lipase mediated oxidations. *Tetrahedron* **1992**, *48*, 4587–4592. [CrossRef]
10. Aouf, C.; Durand, E.; Lecomte, J.; Figueroa-Espinoza, M.C.; Dubreucq, E.; Fulcrand, H.; Villeneuve, P. The use of lipases as biocatalysts for the epoxidation of fatty acids and phenolic compounds. *Green Chem.* **2014**, *16*, 1740–1754. [CrossRef]
11. Schneider, R.d.C.; Lara, L.R.S.; Bitencourt, T.B.; Nascimento, M.d.G.; Nunes, M.R. Chemo-enzymatic epoxidation of sunflower oil methyl esters. *J. Braz. Chem. Soc.* **2009**, *20*, 1473–1477. [CrossRef]
12. Vlcek, T.; Petrovic, Z.S. Optimization of the chemoenzymatic epoxidation of soybean oil. *J. Am. Oil Chem. Soc.* **2006**, *83*, 247–252. [CrossRef]
13. Rüsch gen. Klaas, M.; Warwel, S. Complete and partial epoxidation of plant oils by lipase-catalyzed perhydrolysis. *Ind. Crops Prod.* **1999**, *9*, 125–132. [CrossRef]
14. Rüsch gen. Klaas, M.; Warwel, S. Lipase-catalyzed preparation of peroxy acids and their use for epoxidation. *J. Mol. Catal. A Chem.* **1997**, *117*, 311–319. [CrossRef]
15. Piazza, G.J.; Nuñez, A.; Foglia, T.A. Epoxidation of fatty acids, fatty methyl esters, and alkenes by immobilized oat seed peroxygenase. *J. Mol. Catal. B-Enzym.* **2003**, *21*, 143–151. [CrossRef]
16. Oliw, E.H. Oxygenation of polyunsaturated fatty acids by cytochrome P450 monooxygenases. *Progr. Lipid Res.* **1994**, *33*, 329–354. [CrossRef]
17. Aranda, C.; Olmedo, A.; Kiebist, J.; Scheibner, K.; del Río, J.C.; Martínez, A.T.; Gutiérrez, A. Selective epoxidation of fatty acids and fatty acid methyl esters by fungal peroxygenases. *ChemCatChem* **2018**, *10*, 3964–3968. [CrossRef]
18. Hofrichter, M.; Kellner, H.; Pecyna, M.J.; Ullrich, R. Fungal unspecific peroxygenases: Heme-thiolate proteins that combine peroxidase and cytochrome P450 properties. *Adv. Exp. Med. Biol.* **2015**, *851*, 341–368.
19. Hofrichter, M.; Kellner, H.; Herzog, R.; Karich, A.; Liers, C.; Scheibner, K.; Wambui, V.; Ullrich, R. Fungal peroxygenases: A phylogenetically old superfamily of heme enzymes with promiscuity for oxygen transfer reactions. In *Grand Challenges in Fungal Biotechnology*; Nevalainen, H., Ed.; Springer: Cham, Switzerland, 2020; pp. 369–403.
20. Ullrich, R.; Hofrichter, M. Enzymatic hydroxylation of aromatic compounds. *Cell. Mol. Life Sci.* **2007**, *64*, 271–293. [CrossRef]
21. Gutiérrez, A.; Babot, E.D.; Ullrich, R.; Hofrichter, M.; Martínez, A.T.; del Río, J.C. Regioselective oxygenation of fatty acids, fatty alcohols and other aliphatic compounds by a basidiomycete heme-thiolate peroxidase. *Arch. Biochem. Biophys.* **2011**, *514*, 33–43. [CrossRef]
22. Peter, S.; Kinne, M.; Wang, X.; Ulrich, R.; Kayser, G.; Groves, J.T.; Hofrichter, M. Selective hydroxylation of alkanes by an extracellular fungal peroxygenase. *FEBS J.* **2011**, *278*, 3667–3675. [CrossRef]
23. Aranda, C.; Carro, J.; González-Benjumea, A.; Babot, E.D.; Olmedo, A.; Linde, D.; Martínez, A.T.; Gutiérrez, A. Advances in enzymatic oxyfunctionalization of aliphatic compounds. *Biotechnol. Adv.* **2021**, *51*, 107703. [PubMed]
24. Municoy, M.; González-Benjumea, A.; Carro, J.; Aranda, C.; Linde, D.; Renau-Mínguez, C.; Ullrich, R.; Hofrichter, M.; Guallar, V.; Gutiérrez, A.; et al. Fatty-acid oxygenation by fungal peroxygenases: From computational simulations to preparative regio- and stereo-selective epoxidation. *ACS Catal.* **2020**, *10*, 13584–13595. [CrossRef]
25. González-Benjumea, A.; Carro, J.; Renau, C.; Linde, D.; Fernández-Fueyo, E.; Gutiérrez, A.; Martínez, A.T. Fatty acid epoxidation by *Collariella virescens* peroxygenase and heme-channel variants. *Catal. Sci. Technol.* **2020**, *10*, 717–725. [CrossRef]
26. Carro, J.; González-Benjumea, A.; Fernández-Fueyo, E.; Aranda, C.; Guallar, V.; Gutiérrez, A.; Martínez, A.T. Modulating fatty acid epoxidation *vs* hydroxylation in a fungal peroxygenase. *ACS Catal.* **2019**, *9*, 6234–6242. [CrossRef]
27. Babot, E.D.; del Río, J.C.; Kalum, L.; Martínez, A.T.; Gutiérrez, A. Oxyfunctionalization of aliphatic compounds by a recombinant peroxygenase from *Coprinopsis cinerea*. *Biotechnol. Bioeng.* **2013**, *110*, 2332.
28. Linde, D.; Olmedo, A.; González-Benjumea, A.; Renau, C.; Estévez, M.; Carro, J.; Fernández-Fueyo, E.; Gutiérrez, A.; Martínez, A.T. Two new unspecific peroxygenases from heterologous expression of fungal genes in *Escherichia coli*. *Appl. Environ. Microbiol.* **2020**, *86*, e02899-19. [CrossRef]
29. González-Benjumea, A.; Linde, D.; Carro, J.; Ullrich, R.; Hofrichter, M.; Martínez, A.T.; Gutiérrez, A. Regioselective and stereoselective epoxidation of n-3 and n-6 fatty acids by fungal peroxygenases. *Antioxidants* **2021**, *10*, 1888.

30. Fernández-Fueyo, E.; Aranda, C.; Gutiérrez, A.; Martínez, A.T. Method of Heterologous Expression of Active Fungal Unspecific Peroxygenase in Bacterial Host Cells for Fatty-Acid Epoxidation and Other Oxygenation Reactions. European Patent EP18382514.0, 10 July 2018.
31. Lund, H.; Kalum, L.; Hofrichter, M.; Peter, S. Epoxidation Using Peroxygenase. U.S. Patent 9908860 B2, 6 March 2018.
32. Puigbò, P.; Guzmán, E.; Romeu, A.; Garcia-Vallvé, S. OPTIMIZER: A web server for optimizing the codon usage of DNA sequences. *Nucleic Acids Res.* **2007**, *35*, W126–W131. [CrossRef]
33. Waterhouse, A.; Bertoni, M.; Bienert, S.; Studer, G.; Tauriello, G.; Gumienny, R.; Heer, F.T.; de Beer, T.A.P.; Rempfer, C.; Bordoli, L.; et al. SWISS-MODEL: Homology modelling of protein structures and complexes. *Nucleic Acids Res.* **2018**, *46*, W296–W303.
34. Ullrich, R.; Nuske, J.; Scheibner, K.; Spantzel, J.; Hofrichter, M. Novel haloperoxidase from the agaric basidiomycete *Agrocybe aegerita* oxidizes aryl alcohols and aldehydes. *Appl. Environ. Microbiol.* **2004**, *70*, 4575–4581.
35. Piontek, K.; Strittmatter, E.; Ullrich, R.; Gröbe, G.; Pecyna, M.J.; Kluge, M.; Scheibner, K.; Hofrichter, M.; Plattner, D.A. Structural basis of substrate conversion in a new aromatic peroxygenase: Cytochrome P450 functionality with benefits. *J. Biol. Chem.* **2013**, *288*, 34767–34776. [CrossRef] [PubMed]
36. Laemmli, U.K. Cleavage of structural proteins during the assembly of the head of bacteriophage T_4. *Nature* **1970**, *227*, 680–685. [CrossRef] [PubMed]
37. González-Benjumea, A.; Marques, G.; Herold-Majumdar, O.M.; Kiebist, J.; Scheibner, K.; del Río, J.C.; Martínez, A.T.; Gutiérrez, A. High epoxidation yields of vegetable oil hydrolyzates and methyl esters by selected fungal peroxygenases. *Front. Bioeng. Biotechnol.* **2021**, *8*, 605854. [CrossRef] [PubMed]
38. Pinot, F.; Benveniste, I.; Salaün, J.P.; Loreau, O.; Noël, J.P.; Schreiber, L.; Durst, F. Production in vitro by the cytochrome P450 CYP94A1 of major C18 cutin monomers and potential messengers in plant-pathogen interactions: Enantioselectivity studies. *Biochem. J.* **1999**, *342*, 27–32. [CrossRef]
39. Bormann, S.; Baraibar, A.G.; Ni, Y.; Holtmann, D.; Hollmann, F. Specific oxyfunctionalisations catalysed by peroxygenases: Opportunities, challenges and solutions. *Catal. Sci. Technol.* **2015**, *5*, 2038–2052. [CrossRef]
40. Faiza, M.; Huang, S.F.; Lan, D.M.; Wang, Y.H. New insights on unspecific peroxygenases: Superfamily reclassification and evolution. *BMC Evol. Biol.* **2019**, *19*, 76. [CrossRef]
41. Grogan, G. Hemoprotein catalyzed oxygenations: P450s, UPOs, and progress toward scalable reactions. *JACS Au* **2021**, *1*, 1312–1329. [CrossRef]
42. Hobisch, M.; Holtmann, D.; Gomez de Santos, P.; Alcalde, M.; Hollmann, F.; Kara, S. Recent developments in the use of peroxygenases- Exploring their high potential in selective oxyfunctionalisations. *Biotechnol. Adv.* **2021**, *51*, 107615. [CrossRef]
43. Münch, J.; Püllmann, P.; Zhang, W.; Weissenborn, M.J. Enzymatic hydroxylations of sp3-carbons. *ACS Catal.* **2021**, *11*, 9168–9203. [CrossRef]
44. Beltrán-Nogal, A.; Sánchez-Moreno, I.; Méndez-Sánchez, D.; Gómez de Santos, P.; Hollmann, F.; Alcalde, M. Surfing the wave of oxyfunctionalization chemistry by engineering fungal unspecific peroxygenases. *Curr. Opin. Struct. Biol.* **2022**, *73*, 102342. [CrossRef]
45. Hofrichter, M.; Kellner, H.; Herzog, R.; Karich, A.; Kiebist, J.; Scheibner, K.; Ullrich, R. Peroxide-mediated oxygenation of organic compounds by fungal peroxygenases. *Antioxidants* **2022**, *11*, 163. [CrossRef] [PubMed]
46. Wang, Y.; Lan, D.; Durrani, R.; Hollmann, F. Peroxygenases *en route* to becoming dream catalysts. What are the opportunities and challenges? *Curr. Opin. Chem. Biol.* **2017**, *37*, 1–9. [CrossRef] [PubMed]

antioxidants

MDPI

Article

SUPPLEMENTARY MATERIALS

Engineering *Collariella virescens* Peroxygenase for Epoxides Production from Vegetable Oil

Dolores Linde [1,†], Alejandro González-Benjumea [2,†], Carmen Aranda [3], Juan Carro [1], Ana Gutiérrez [2] and Angel T. Martínez [1,*]

[1] Centro de Investigaciones Biológicas "Margarita Salas" (CIB), CSIC, E-28040 Madrid, Spain; lolalinde@cib.csic.es (D.L.); jcarro@cib.csic.es (J.C.)
[2] Instituto de Recursos Naturales y Agrobiología de Sevilla (IRNAS), CSIC, E-41012 Seville, Spain; a.g.benjumea@irnas.csic.es (A.G.-B.); anagu@irnase.csic.es (A.G.)
[3] Johnson Matthey, Cambridge Science Park U260, Cambridge CB4 0FP, UK; carmen.aranda@matthey.com
* Correspondence: atmartinez@cib.csic.es; Tel.: +34-918373112
† These authors contributed equally to this work.

This Supplementary Materials includes: Kinetic constants for substrate oxidation by native r*Cvi*UPO and variants in the presence of 1 mM and 24 mM H_2O_2 (**Tables S1** and **S2,** respectively); SDS-PAGE of purified native r*Cvi*UPO and variants (**Figure S1**); UV-visible spectra of resting states and CO complexes of r*Cvi*UPO and variants (**Figure S2**); Effect of pH on the oxidation of different substrates (**Figure S3**); Kinetic curves for different UPO reducing substrates and H_2O_2 (**Figure S4**); GC-MS analyses of oleic acid, linoleic, and α–linolenic acids reactions with *Cvi*UPO and four heme channel variants (**Figures S5-S7**, respectively); and Chiral HPLC analysis of oleic acid epoxide (**Figure S8**).

Table S1. Kinetic constants for substrate (veratryl and benzyl alcohols, naphthalene and ABTS) oxidation by the native *Cvi*UPO and variants (F88A, T158A, F88A/T158A and 6Ala) in the presence of 1 mM H_2O_2.

	k_{cat} (s^{-1})	K_m (μM)	k_{cat}/K_m (s^{-1} mM^{-1})	ki(μM)	nH
Veratryl alcohol					
Native	2.24 ± 0.03	2,940± 159	0.75 ± 0.03	-	-
F88A	2.65 ± 0.19	1,050 ± 159	2.51 ± 0.12	-	-
T158A	1.51 ± 0.03	820 ± 100	1.84 ± 0.19	-	-
F88A/T158A	2.40 ± 0.10	1,720 ± 340	1.38 ± 0.23	-	-
6Ala	0	-	0	-	-
Naphthalene					
Native	1.09 ± 0.07	450 ± 70	2.42 ± 0.24	-	-
F88A	3.68 ± 0.17	435 ± 563	8.47 ± 0.74	-	-
T158A	1.28 ± 0.04	180 ± 14	7.17 ± 0.42	-	-
F88A/T158A	1.62 ± 0.05	100 ± 12	16.20 ± 1.50	-	-
6Ala	0	-	0	-	-
ABTS					
Native	157.0 ± 3.0	239 ± 8	656 ± 26	7,860 ± 680	-
F88A	16.3 ± 0.8	48 ± 7	334 ± 54	98,400 ± 11,200	-
T158A	163.0 ± 24.0	260 ± 60	627 ± 171	811 ± 204	-
F88A/T158A	5.3 ± 0.3	7 ± 2	768 ± 197	-	-
6Ala	5.2 ± 0.1	83 ± 11	62 ± 7	-	-
Benzyl alcohol					
Native	63.0 ± 2.3	7,050 ± 570	8.92 ± 0.42	-	1.6 ± 0.1
F88A	20.1 ± 1.0	5,420 ± 91	3.71 ± 0.66	47,600 ± 9,100	-
T158A	128.1 ± 6.6	8,970 ± 1460	14.28 ± 2.37	-	1.5 ± 0.2
F88A/T158A	8.5 ± 0.5	809 ± 138	10.70 ± 1.89	32,400 ± 6,100	-
6Ala	9.6 ± 1.5	4,300 ± 2400	2.20 ± 1.60	-	-

The kinetic constants were measured in 100 mM acetate (veratryl alcohol and ABTS), 100 mM Tris (benzyl alcohol) or 100 mM tartrate (naphthalene) at the optimal pH for each enzyme-substrate couple

Table S2. Kinetic constants for substrate (veratryl and benzyl alcohols, naphthalene, and ABTS) oxidation by native r*Cvi*UPO and variants (F88A, T158A, F88A/T158A and 6Ala) in the presence of 24 mM H_2O_2.

	k_{cat} (s^{-1})	K_m (μM)	k_{cat}/K_m ($s^{-1}\cdot mM^{-1}$)	k_i (μM)
Veratryl alcohol				
Native	5.7 ± 0.2	20,800 ± 2,300	0.27 ± 0.03	-
F88A	11.1 ± 0.3	4,740 ± 480	2.34 ± 0.24	-
T158A	6.5 ± 0.4	37,500 ± 5,500	0.17 ± 0.02	-
F88A/T158A	43.5 ± 1.8	15,000 ± 2,000	2.89 ± 0.39	-
6Ala	3.7 ± 0.3	3,590 ± 1,040	1.03 ± 0.31	-
Naphthalene				
Native	2.3 ± 0.3	648 ± 235	3.5 ± 0.8	-
F88A	13.9 ± 0.91	239 ± 51	58.1 ± 12.9	-
T158A	1.8 ± 0.1	160 ± 37.6	11.2 ± 2.7	-
F88A/T158A	39.8 ± 2.4	151 ± 33	263.0 ± 38.0	-
6Ala	6.1 ± 0.7	360 ± 123	16.9 ± 6.1	-
ABTS				
Native	237 ± 19	576 ± 150	411 ± 86.8	-
F88A	630 ± 54	225 ± 44	2,800 ± 597	6,610 ± 1,900
T158A	200 ± 8	590 ± 76	339 ± 45.7	-
F88A/T158A	660 ± 23	153 ± 23	4,310 ± 670	-
6Ala	12 ± 1	391 ± 42	30 ± 3	-
Benzyl alcohol				
Native	59 ± 2	8,020 ± 1,030	7.3 ± 1.0	-
F88A	210 ± 41	25,700 ± 10,500	8.2 ± 3.7	-
T158A	380 ± 51	45,300 ± 10,500	8.4 ± 2.2	-
F88A/T158A	297 ± 31	9,490 ± 2,840	31.3 ± 9.9	-
6Ala	16 ± 1	3,850 ± 220	4.1 ± 0.3	-

The kinetics constants were measured in 100 mM acetate (veratryl alcohol and ABTS), 100 mM Tris (benzyl alcohol) or 100 mM tartrate (naphthalene) at the optimal pH for each enzyme-substrate couple.

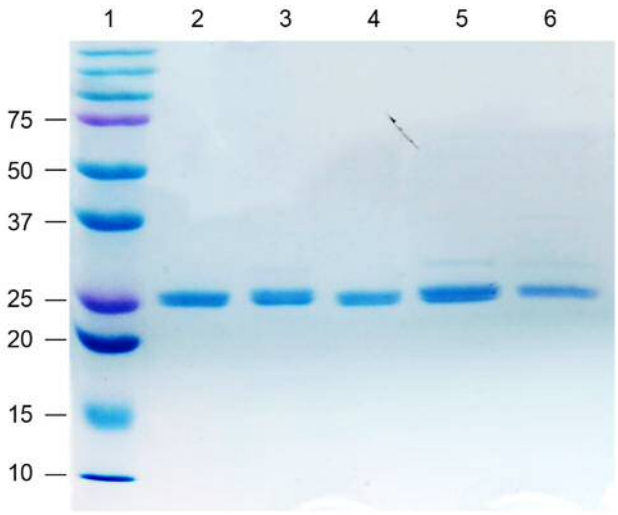

Figure S1. SDS-PAGE of purified native r*Cvi*UPO (*lane 2*) and variants F88A (*lane 3*), T158A (*lane 4*), F88A/T158A (*lane 5*) and 6Ala (*lane 6*). Molecular-mass markers are indicated in kDa (*lane 1*).

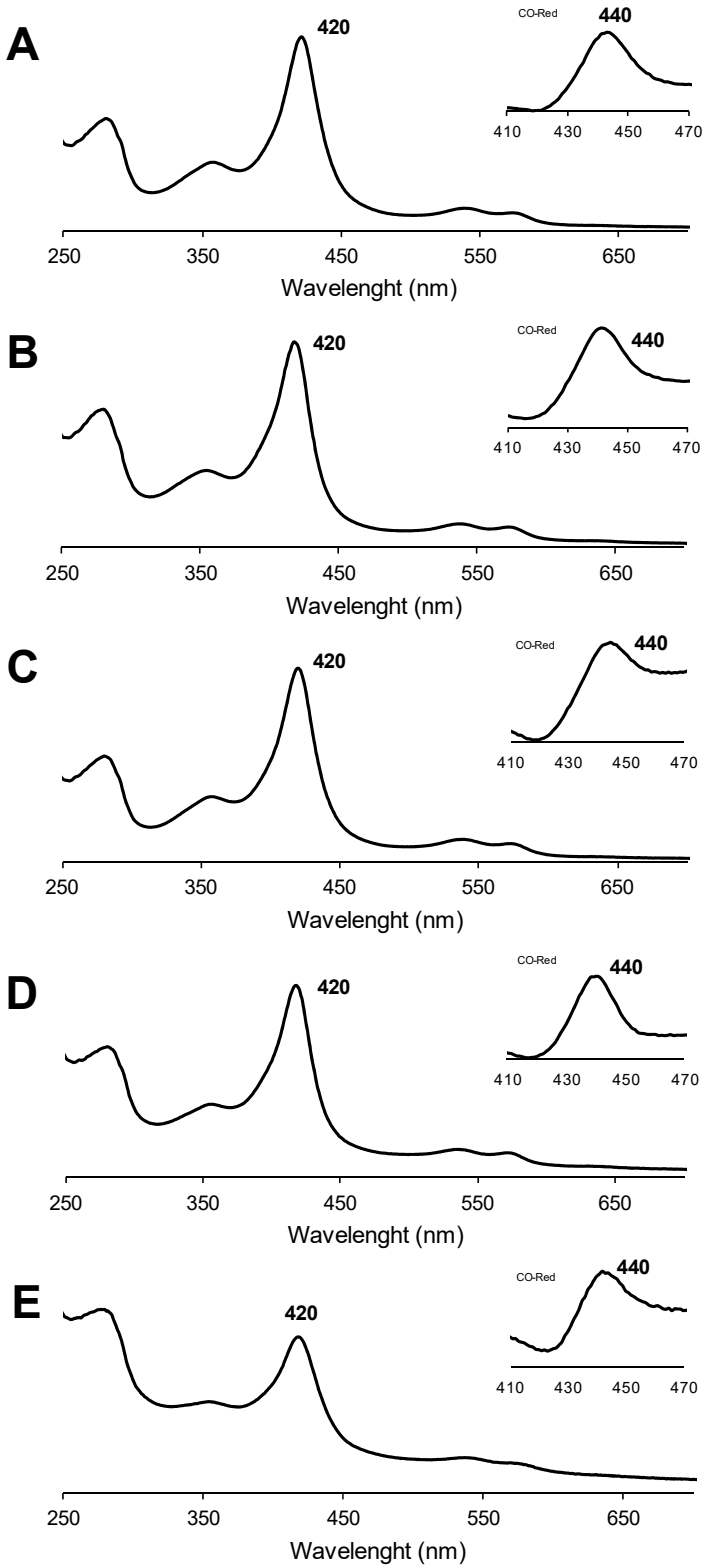

Figure S2. UV-visible spectra of resting states (main panels) and CO complexes (insets) of native r*Cvi*UPO (**A**) and its F88A (**B**), T158A (**C**), F88A/T158A (**D**) and 6Ala (**E**) heme-channel variants. The resting-state Soret band (around 420 nm in the main panels) is characteristically displaced (at around 440 nm), in the complexes between the reduced enzyme and CO, as shown in the difference spectra included in the insets (obtained by subtracting the spectrum of the reduced enzyme).

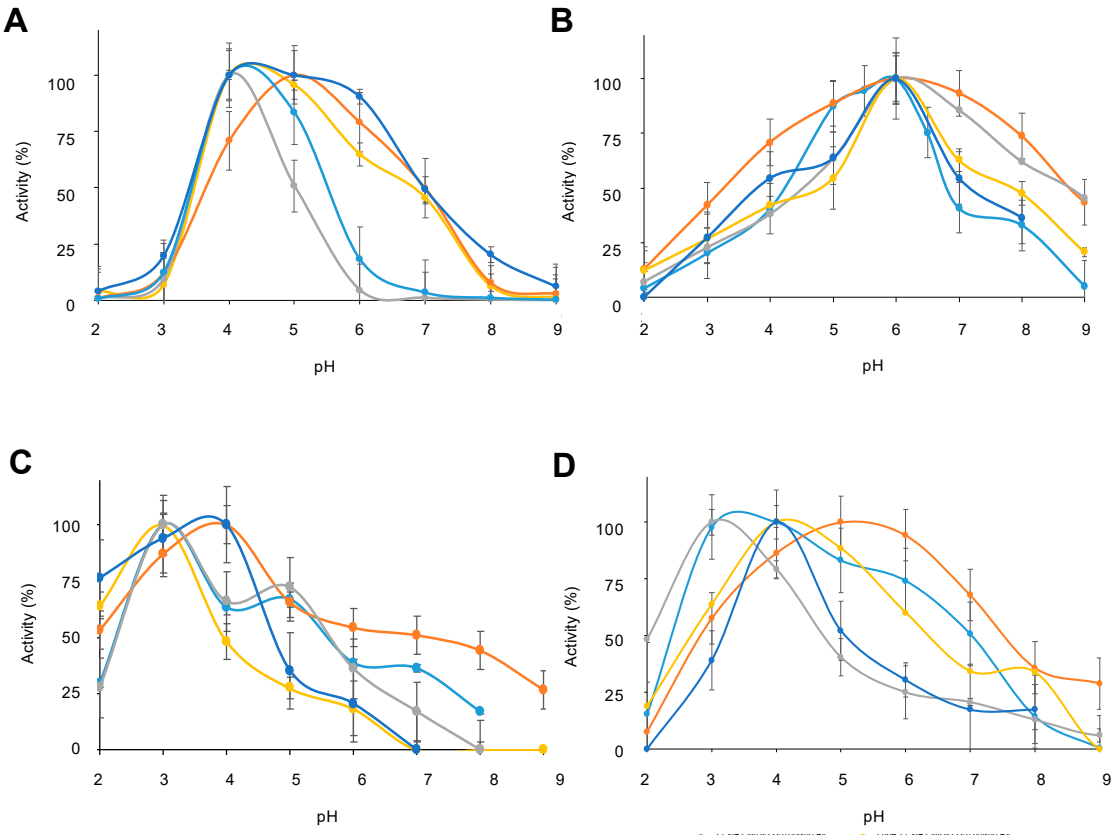

Figure S3. Effect of pH on oxidation of four UPO substrates. Relative activity of native r*Cvi*UPO (*cyan*) and its F88A (*orange*), T158A (*gray*), F88A/T158A (*yelow*) and 6Ala (*dark blue*) variants oxidizing 2 mM ABTS (**A**), 10 mM benzyl alcohol (**B**), 1 mM naphthalene (**C**) and 10 mM veratryl alcohol (**D**) at different pH values (measured in 50 mM Britton-Robinson buffer, pH 2-9). Bars represent the standard deviations of the means of three measurements.

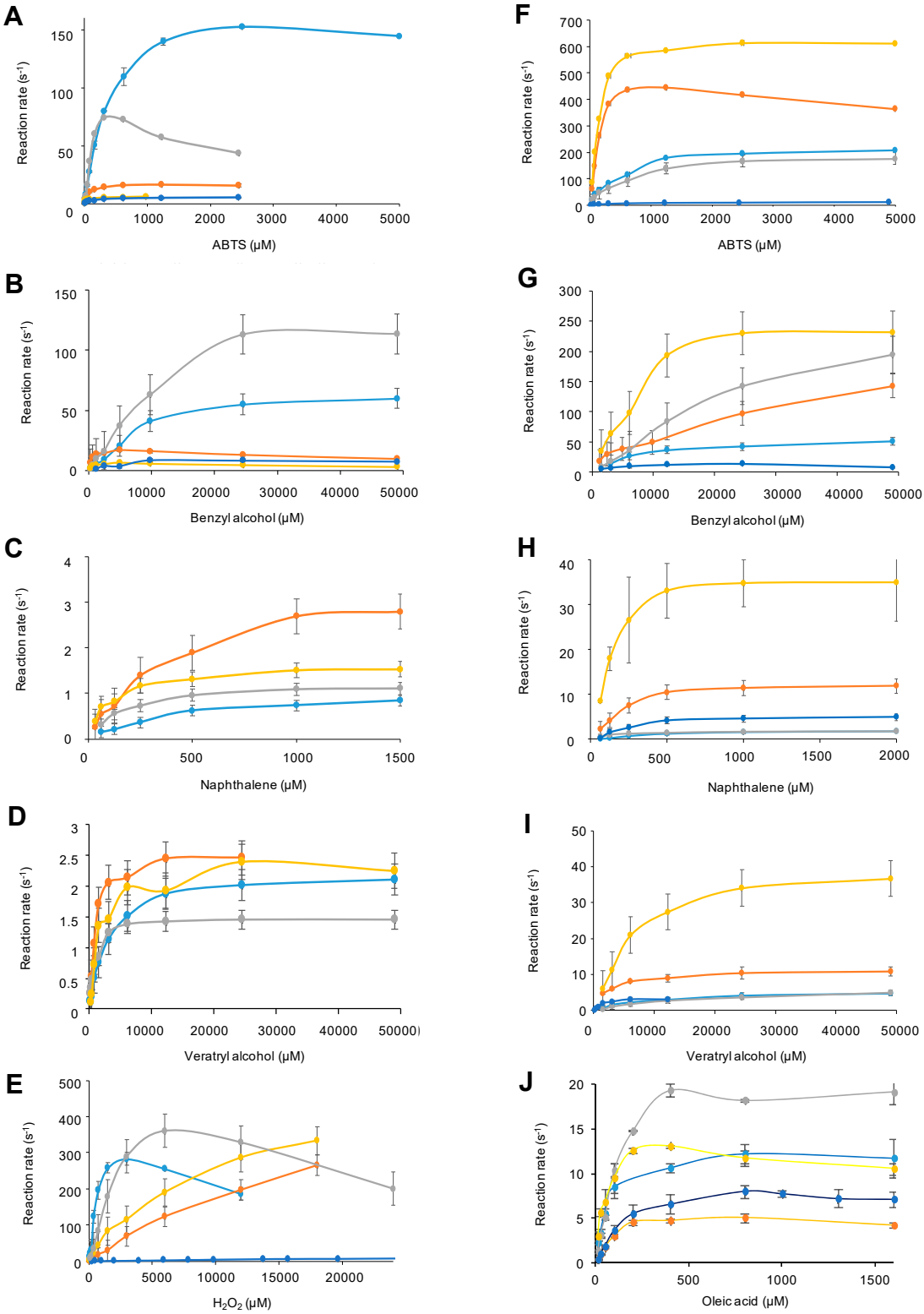

Figure S4. Kinetic curves for UPO reducing substrates and H_2O_2. The reaction rates of native r*Cvi*UPO (*cyan*) and its F88A (*orange*), T158A (*gray*), F88A/T158A (*yelow*) and 6Ala (*dark blue*) variants with different concentrations of ABTS (**A,F**), benzyl alcohol (**B,G**), naphthalene (**C,H**), veratryl alcohol (**D,I**), H_2O_2 (**E**) and oleic acid (**J**) were measured using 1 mM (**A-D**) or 24 mM (**F-J**) H_2O_2, and 2.5 mM ABTS (**E**) as cosubstrate. Bars represent the standard deviations of the means of three measurements.

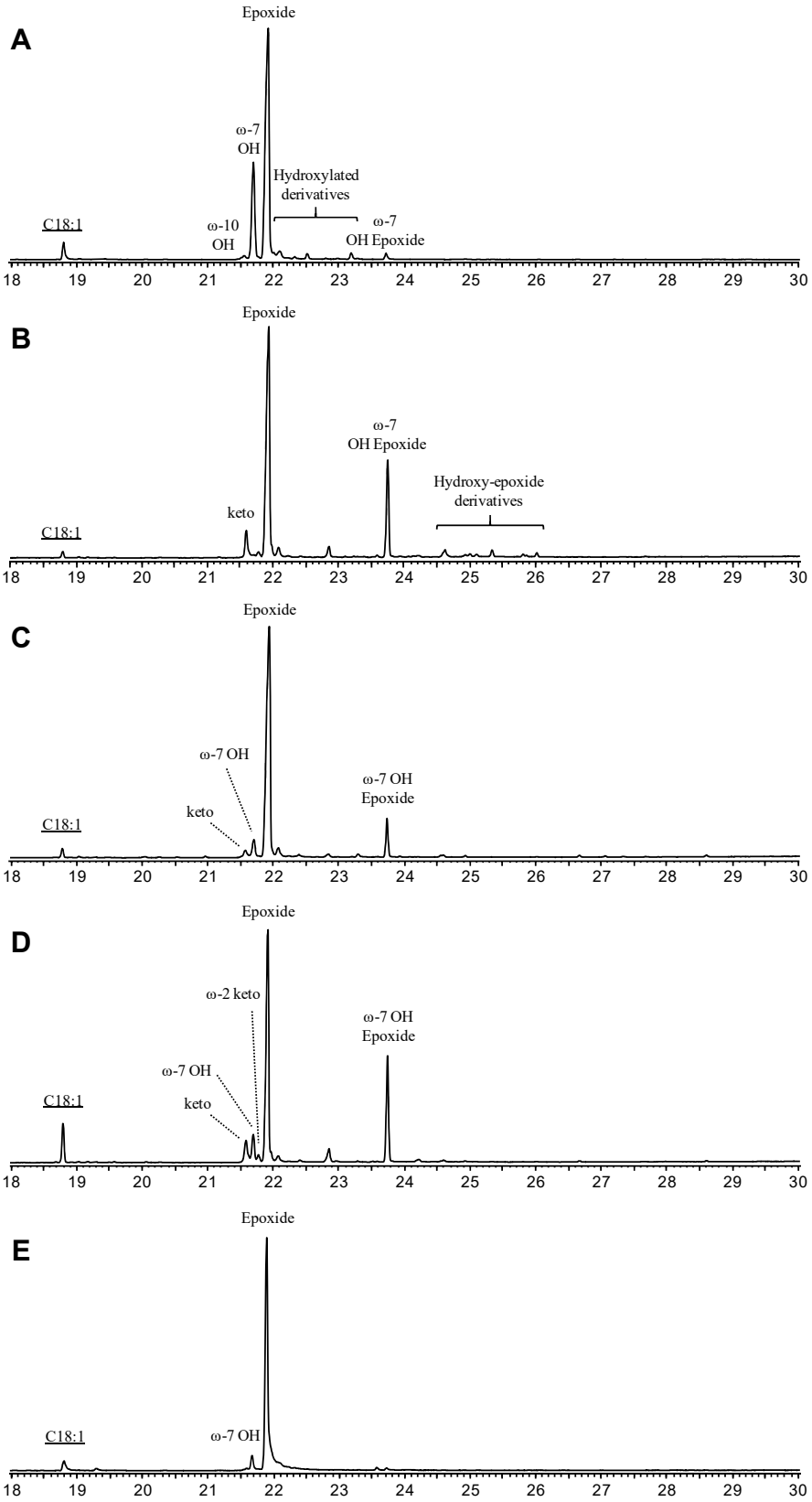

Figure S5. GC-MS analysis of oleic acid (C18:1) reactions with *Cvi*UPO (**A**) and its F88A (**B**), T158A (**C**), F88A/T158A (**D**) and 6Ala (**E**) variants. Reaction mixtures containing 0.1 mM substrate, 1.4 μM enzyme and 1.25 mM H_2O_2 were incubated for 30 min, extracted, and derivatized before GC-MS analysis.

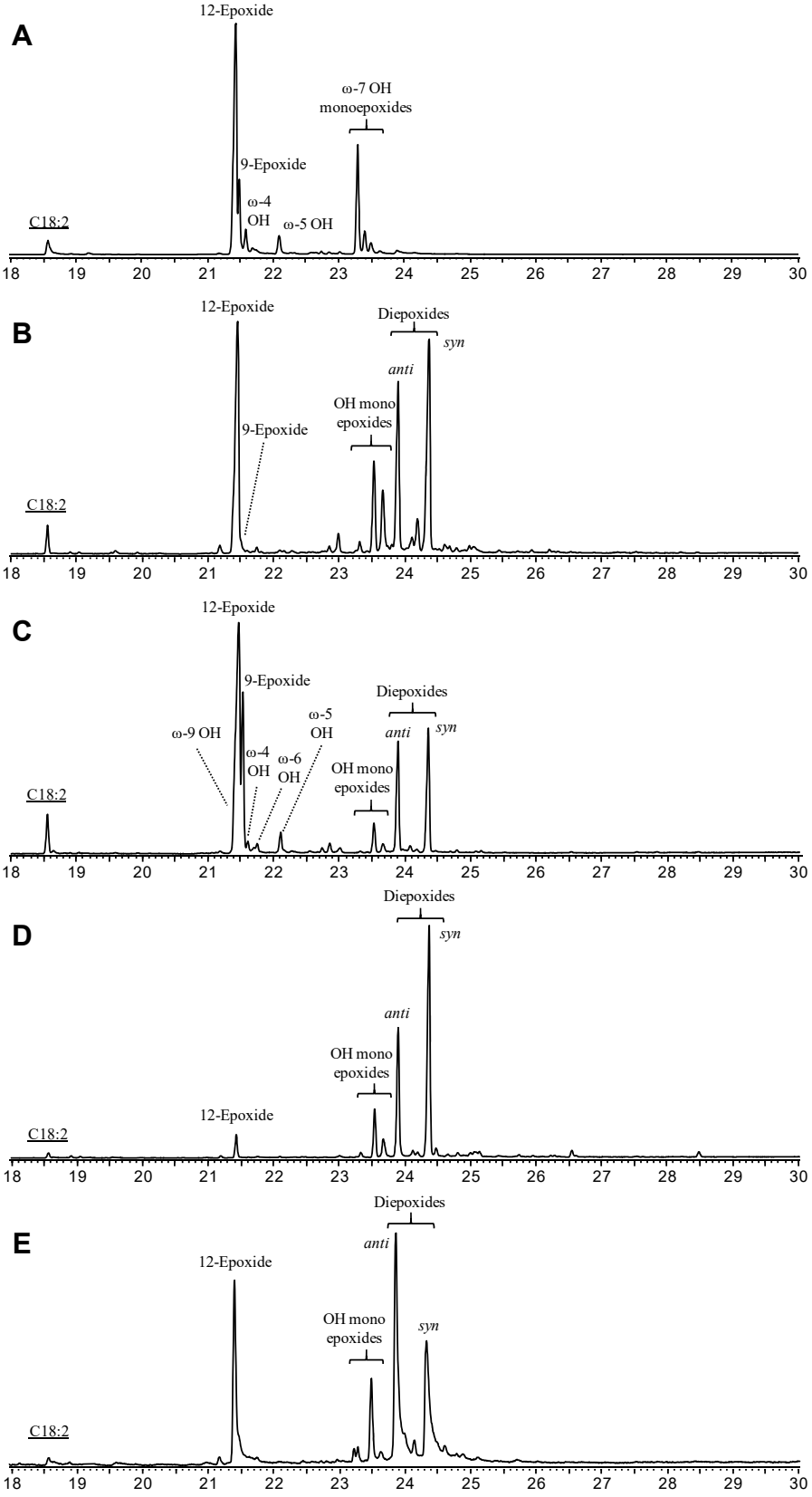

Figure S6. GC-MS analysis of linoleic acid (C18:2) reactions with *Cvi*UPO (**A**) and its F88A (**B**), T158A (**C**), F88A/T158A (**D**) and 6Ala (**E**) variants. Reaction mixtures containing 0.1 mM substrate, 1.4 μM enzyme and 1.25 mM H_2O_2 were incubated for 30 min, extracted, and derivatized before GC-MS analysis.

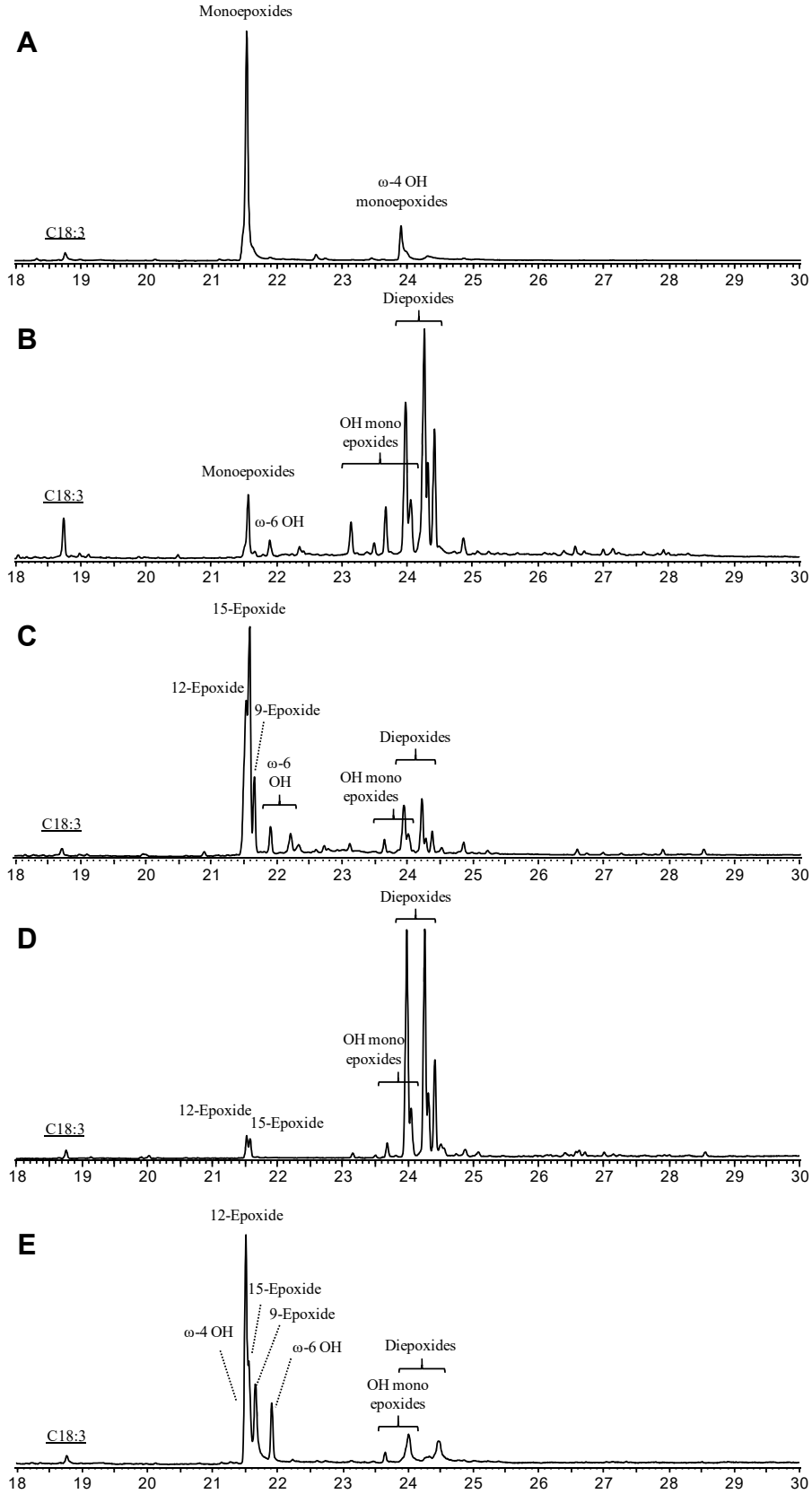

Figure S7. GC-MS analysis of α-linolenic acid (C18:3) reactions with *Cvi*UPO (**A**) and its F88A (**B**), T158A (**C**), F88A/T158A (**D**) and 6Ala (**E**) variants. Reaction mixtures containing 0.1 mM substrate, 1.4 μM enzyme and 1.25 mM H_2O_2 were incubated for 30 min, extracted, and derivatized before GC-MS analysis.

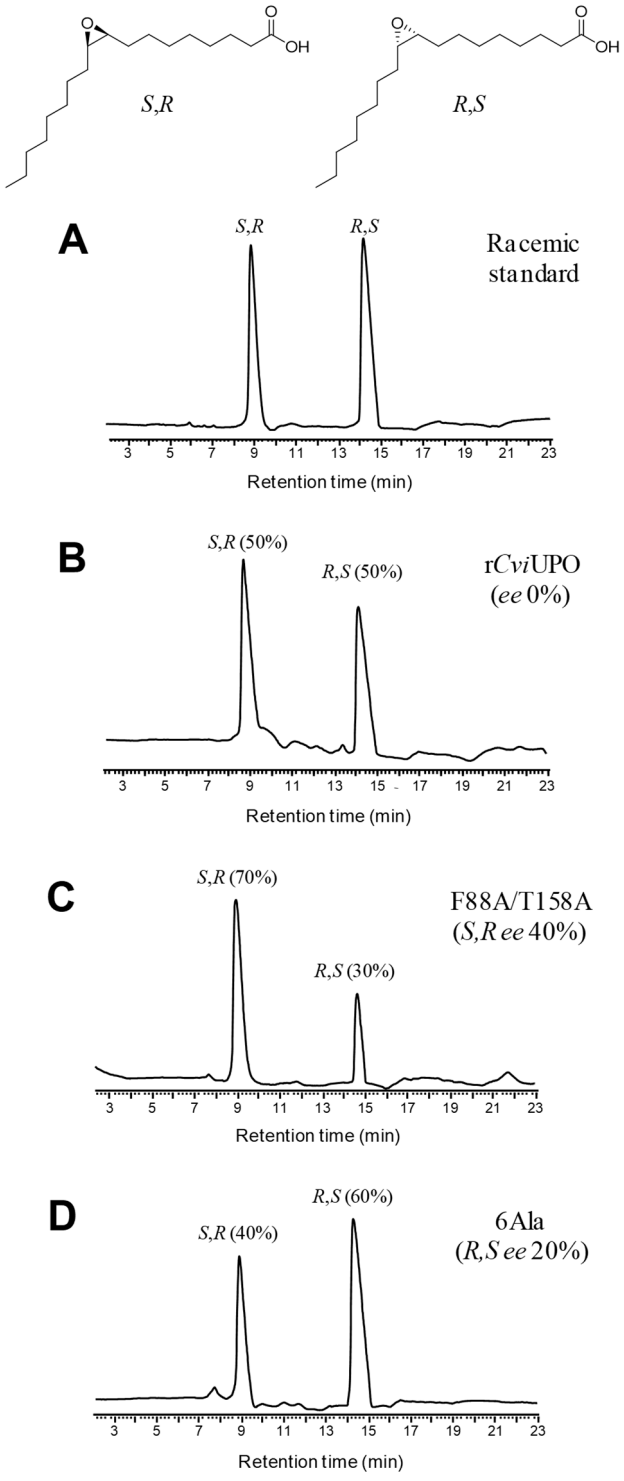

Figure S8. Chiral HPLC analysis of oleic acid epoxidation with native r*Cvi*UPO (**B**) and its F88A/T158A (**C**) and 6Ala (**D**) variants, compared with a racemic epoxyoleic acid standard (**A**), with indication of the relative abundance of the *S,R* and *R,S* enantiomers and the resulting *ee* values.